EPJ manuscript No.
(will be inserted by the editor)

Evaluation of the polarization observables I^S and I^C in the reaction $\gamma p \to \pi^0 \eta p$

M. Döring[1], E. Oset[2], and Ulf-G. Meißner[1,3,4]

[1] Institut für Kernphysik and Jülich Center for Hadron Physics, Forschungszentrum Jülich, D-52425 Jülich, Germany [a]
[2] Departamento de Física Teórica and IFIC, Centro Mixto Universidad de Valencia-CSIC, Institutos de Investigación de Paterna, Aptdo. 22085, 46071 Valencia, Spain [b]
[3] Institute for Advanced Simulation, Forschungszentrum Jülich, D-52425 Jülich, Germany
[4] Helmholtz-Institut für Strahlen- und Kernphysik (Theorie) and Bethe Center for Theoretical Physics, Universität Bonn, Nußallee 14-16, D-53115 Bonn, Germany [c]

FZJ-IKP-TH-2010-6, HISKP-TH-10/07

Abstract. We evaluate the polarization observables I^S and I^C for the reaction $\gamma p \to \pi^0 \eta p$, using a chiral unitary framework developed earlier. The I^S and I^C observables have been recently measured for the first time by the CBELSA/TAPS collaboration. The theoretical predictions of I^S and I^C, given for altogether 18 angle dependent functions, are in good agreement with the measurements. Also, the asymmetry $d\Sigma/d\cos\theta$ evaluated here agrees with the data. We show the importance of the $\Delta(1700)$ D_{33} resonance and its S-wave decay into $\eta\Delta(1232)$. The result can be considered as a further confirmation of the dynamical nature of this resonance. At the highest energies, deviations of the predictions from the data start to become noticeable, which leaves room for additional processes and resonances such as a $\Delta(1940)$ D_{33}. We also point out how to further improve the calculation.

PACS. 25.20.Lj Photoproduction reactions – 13.60.Le Meson production – 13.75.Gx Pion-baryon interactions – 14.20.Gk Baryon resonances with S=0

1 Introduction

The photoproduction of meson pairs is proving to be a rich field allowing us to widen our understanding of hadron dynamics and hadron structure. Following much work devoted to the photoproduction of two pions in the last decade, both experimental [1,2,3,4,5,6,7,8,9,10,11,12,13,14,15,16,17] and theoretical [18,19,20,21,22,23,24,25,26,27,28,29], time is ripe to investigate $\pi^0\eta$ photoproduction, which has brought us some surprises.

$\pi^0\eta$ photoproduction has been studied experimentally, and unpolarized and differential cross sections are reported in Refs. [30,31,32,33,34]. Polarization observables are reported in Refs. [31,35,36,37]. The reaction was studied theoretically in Refs. [38,39]. The result of Ref. [39] was actually a prediction, though preliminary experimental results from [40] were available at that time. Following this work, other more recent papers have tackled the problem theoretically based on models [41] or partial wave analysis of the data [42,43]. In the work of [39] the process turned out to be dominated at low energies by the excitation of the $\Delta(1700)$, which then decays into $\eta\Delta$, with the Δ subsequently decaying into πN. Predictions of the cross section were made possible because the $\Delta(1700)$ happens to be one of the dynamically generated resonances from the interaction of pseudoscalar mesons with the baryons of the Δ decuplet [44,45]. The couplings of the resonance to the different channels were calculated in [45] and these, together with the experimental knowledge of the decay of the $\Delta(1700)$ into γN, allowed one to obtain absolute numbers for the cross section which agree with present measurements.

In Ref. [46] the radiative decay width of the $\Delta(1700) \to \gamma N$ could be predicted, because the photon coupling to the mesons and baryons that constitute this resonance are all well known. The result is in agreement with the phenomenologically known values [47] from data analyses which are used in Refs. [31,39,48] for the $\gamma p \to \pi^0 \eta p$ reaction. In Ref. [46], also the πN channel, that couples weakly to the $\Delta(1700)$ in D-wave, has been included in the unitary model, and a good fit to the πN phase shifts could be obtained.

The theoretical framework from Refs. [39,45] is quite predictive since another one of the couplings of the $\Delta(1700)$ resonance is to the $K\Sigma(1385)$ state and one can evaluate the total and differential cross sections for the reaction

[a] e-mail: m.doering@fz-juelich.de
[b] e-mail: oset@ific.uv.es
[c] e-mail: meissner@hiskp.uni-bonn.de

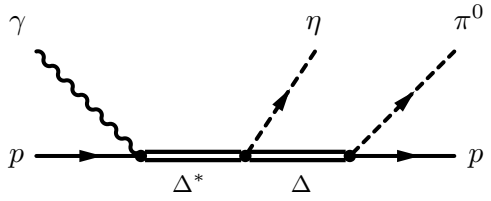

Fig. 1. Tree level process from the decay of the $\Delta(1700)$ to $\eta\Delta(1232)$. This is the dominant process (for the full list of processes, see Ref. [39]). The complex $\Delta(1700) \to \eta\Delta(1232)$ coupling is a prediction within the chiral unitary framework.

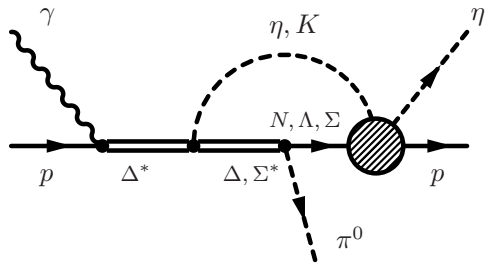

Fig. 2. Processes with $\Delta(1700)\eta\Delta$ and $\Delta(1700)K\Sigma(1385)$ couplings and $\pi^0 S_{11}(\eta p)$ final states. These processes give a major contribution to the $\pi^0 N(1535)$ final state.

$\gamma p \to K^0\pi^0\Sigma^+$ [39], which agree with the measurements published in Ref. [49].

From the list of the underlying processes of the theoretical framework of Ref. [39], we show here only those of Figs. 1 and 2, which involve the $\Delta(1700)\eta\Delta$ and $\Delta(1700)K\Sigma(1385)$ vertices predicted from the chiral unitary amplitudes [45]. These processes give the largest contributions to the $\eta\Delta$ and $\pi^0 S_{11}(\eta p)$ final states. The latter appears from the unitarization of the meson-baryon amplitude in which the $N(1535)$ appears dynamically generated. There are, however, also processes given by S-channel resonance exchange taken from the $\gamma N \to \pi\pi N$ Valencia model of Ref. [26]. Furthermore, there are contributions from Kroll-Ruderman and meson pole terms, contributions from the normal and anomalous magnetic moments of the baryons, and combinations of those processes. All free constants that appear in the model have been fixed from other processes, thus the results of Ref. [39] can be regarded as predictions.

The model resulting from Figs. 1 and 2 is gauge invariant. This is so since the $\gamma N\Delta(1700)$ coupling is obtained from the experimental data through an expression which is manifestly gauge invariant [see Eqs. (72,73) of Ref. [23]]. The dominance of the $\Delta(1700)$ excitation is also corroborated by recent analyses of the data [41,42,43,50]. The full model of Ref. [39] contains other terms, apart from the largely dominant ones of Figs. 1, 2. Some of these minor terms considered in Ref. [39] involve a photon coupling to a loop and a meson baryon scattering amplitude obtained using the chiral unitary approach (see for instance Fig. 7 of [39]). It was proved in Refs. [51,52] (see also [53]) that due to the series of diagrams implicit in the Bethe Salpeter expansion of the scattering matrix, gauge invariance of the model requires that the photon is coupled to particles and vertices in the intermediate loops and not just only to the last loop.

Although formally needed for the test of gauge invariance, these terms are generally small. They vanish in the limit of low photon momentum, and induce corrections of order $(p_\gamma/2M_p)^2$, which must be evaluated in each case if p_γ is not small. In the work of [39] they were evaluated and found to induce corrections of the order of 5% of the contribution of the term with the photon coupled to the last loop considered in Fig. 7 of [39]. Since this latter term represents a small correction compared to the contribution of the diagrams of Figs. 1 and 2 here, neglecting the gauge fixing terms of [51,52,53] in the present case, corresponds to neglecting small corrections to small terms and which were safely disregarded in Ref. [39] and in the present work.

The resulting theoretical framework also allows to correlate up to eleven different cross sections induced by photons or pions and this work has been reported in Ref. [48]. All these successful predictions strongly support the claim of the $\Delta(1700)$ being a dynamically generated resonance. Yet, there are more challenges for this approach, and the polarization observables of the $\gamma p \to \pi^0\eta p$ reaction are some of them. The polarization asymmetry Σ was measured in Ref. [31] and in the same work the approach of Ref. [39] was used to describe the data. It was found there that the theoretical framework made the right predictions and that the presence of the $\Delta(1700)$ was essential for this success.

The recent work of Ref. [36] presents another challenge since new observables are measured, i.e, the I^S and I^C polarizations as a function of the ϕ^* angle between the decay plane and the reaction plane [cf. Fig. 3].

The purpose of the present work is to evaluate these new polarization observables, and also $d\Sigma/d\cos\theta$ measured recently [35], in order to test the theoretical framework of Ref. [39] and hence the nature of the $\Delta(1700)$. As we shall see, these observables are well reproduced and one can see that in the absence of the $\Delta(1700)$ term in the amplitude the results grossly deviate from experiment, showing once again the essential role played by this resonance in the $\gamma p \to \pi^0\eta p$ reaction and providing further support for the idea of this resonance as being dynamically generated.

The paper is organized as follows: In sec. 2 we present the formalism, followed by the presentation of our results in sec. 3. We end with a short summary.

2 Formalism

2.1 Reaction geometry

Fig. 3 shows the geometry of the reaction $\gamma p \to \pi^0\eta p$. All quantities are defined in the overall center-of-mass (c.m.) system. In the figure, the configuration is chosen in which the proton is the spectator; the two other cases of the π^0

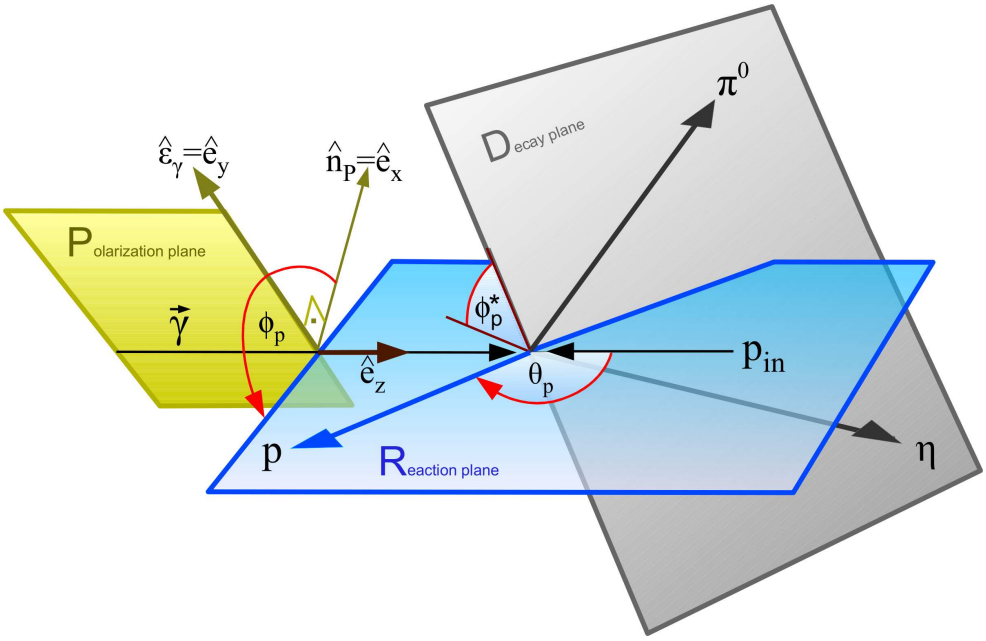

Fig. 3. Definition of the angles ϕ and ϕ^* (center-of-mass-frame). The polarization plane (P) is defined by the photon momentum $\boldsymbol{k}_\gamma$ and the polarization vector $\hat{\boldsymbol{\epsilon}}_\gamma$. Here, the photon is polarized in the vertical plane, $\hat{\boldsymbol{\epsilon}}_\gamma || \hat{\boldsymbol{e}}_y$ and then the normal $\hat{\boldsymbol{n}}_P$ of the polarization plane is $\hat{\boldsymbol{n}}_P || \hat{\boldsymbol{e}}_x$. The reaction plane (R) is defined by $\boldsymbol{k}_\gamma$ and the momentum of the spectator, here the recoiling (final state) proton with $\boldsymbol{p}_p$. The decay plane (D) is defined by the momenta of the final states, given by $\boldsymbol{p}_p$ and the π^0 and η momenta $\boldsymbol{p}_{\pi^0}$ and $\boldsymbol{p}_\eta$. The polar angle of the spectator/recoiling particle is denoted as θ_p. The initial proton is given by $\boldsymbol{p}_{in}$.

and η being the spectator are defined analogously. The definitions given here agree with those of the CBELSA/TAPS experiment [36,54].

The photon momentum is in the z direction, $\boldsymbol{k}_\gamma || \hat{\boldsymbol{e}}_z$. Its linear polarization is chosen in the y direction, i.e. the polarization vector is $\hat{\boldsymbol{\epsilon}}_\gamma || \hat{\boldsymbol{e}}_y$. This geometry is usually referred to as polarization in the "vertical plane". Then, for the normal $\hat{\boldsymbol{n}}_P$ of the polarization plane P, $\hat{\boldsymbol{n}}_P || \hat{\boldsymbol{e}}_x$.

The reaction plane R is defined by the momentum of the incoming photon $\boldsymbol{k}_\gamma$ and the momentum of the spectator, here the recoiling (final state) proton with momentum $\boldsymbol{p}_p$. The angle ϕ is defined as the angle between the reaction plane and the normal to the polarization plane. This azimuthal angle is counted in the xy plane counterclockwise starting from the direction $\hat{\boldsymbol{e}}_x$. For example, for a spectator proton of three momentum $\boldsymbol{p}_p = (0, y, z)$ (y, z arbitrary), $\phi_p = +90^0$. The ϕ angles for the cases of π^0 and η spectators are denoted as ϕ_{π^0} and ϕ_η in the following. The normal of the reaction plane R is given by

$$\hat{\boldsymbol{n}}_R^p = \frac{\hat{\boldsymbol{e}}_z \times \boldsymbol{p}_p}{|\hat{\boldsymbol{e}}_z \times \boldsymbol{p}_p|}, \hat{\boldsymbol{n}}_R^{\pi^0} = \frac{\hat{\boldsymbol{e}}_z \times \boldsymbol{p}_{\pi^0}}{|\hat{\boldsymbol{e}}_z \times \boldsymbol{p}_{\pi^0}|}, \hat{\boldsymbol{n}}_R^\eta = \frac{\hat{\boldsymbol{e}}_z \times \boldsymbol{p}_\eta}{|\hat{\boldsymbol{e}}_z \times \boldsymbol{p}_\eta|}, \quad (1)$$

where the index of $\hat{\boldsymbol{n}}_R$ indicates the spectator particle.

The decay plane D is defined by the momenta of the three final state particles p, π^0, η which all lie in one plane due to momentum conservation. The normal $\hat{\boldsymbol{n}}_D$ of the decay plane D defines the orientation,

$$\hat{\boldsymbol{n}}_D^p = \frac{\boldsymbol{p}_{\pi^0} \times \boldsymbol{p}_\eta}{|\boldsymbol{p}_{\pi^0} \times \boldsymbol{p}_\eta|}, \hat{\boldsymbol{n}}_D^{\pi^0} = \frac{\boldsymbol{p}_p \times \boldsymbol{p}_\eta}{|\boldsymbol{p}_p \times \boldsymbol{p}_\eta|}, \hat{\boldsymbol{n}}_D^\eta = \frac{\boldsymbol{p}_{\pi^0} \times \boldsymbol{p}_p}{|\boldsymbol{p}_{\pi^0} \times \boldsymbol{p}_p|}. \quad (2)$$

ϕ^* is the angle between the normals of the R and the D planes, unambiguously defined as

$$\phi_i^* = \begin{cases} \arccos(\hat{\boldsymbol{n}}_D^i \cdot \hat{\boldsymbol{n}}_R^i) & \text{if } (\hat{\boldsymbol{n}}_D^i \times \hat{\boldsymbol{n}}_R^i) \cdot \boldsymbol{p}_i > 0 \\ 2\pi - \arccos(\hat{\boldsymbol{n}}_D^i \cdot \hat{\boldsymbol{n}}_R^i) & \text{otherwise} \end{cases} \quad (3)$$

for all three cases $i = p, \pi^0, \eta$. Note that $\hat{\boldsymbol{n}}_D^p \times \hat{\boldsymbol{n}}_R^p$ and $\boldsymbol{p}_p$ are parallel, because $\boldsymbol{p}_p$ lies in both the R and the D planes (analogously for the π^0 and η spectator cases). As we will also evaluate the beam asymmetry $d\Sigma/d\cos\theta$ measured in Ref. [35], the polar angle θ_p of the spectator is also shown in Fig. 3.

2.2 Monte Carlo evaluation

In this section, the details of the Monte Carlo evaluation of the three-body phase space are presented. With this method, different observables can be easily evaluated which would otherwise require a tedious re-parameterization of the amplitude for every new measured observable. The total energy is $\sqrt{s} \equiv W$.

The total cross section of the $\gamma p \to \pi^0 \eta p$ reaction in Ref. [39], Eq. (47), is written as an integral over the $\pi^0 p$ invariant mass, with one of the phase space integrals evaluated in the $\pi^0 p$ rest frame,

$$\sigma = \int_{m_{\pi^0}+M_p}^{\sqrt{s}-m_\eta} dM_I(\pi^0 p) \frac{d\sigma}{dM_I(\pi^0 p)} \quad (4)$$

with

$$\frac{d\sigma}{dM_I(\pi^0 p)} = \frac{1}{4(2\pi)^5} \frac{M_p M_f}{s - M_p^2} \frac{\tilde{p}_\pi p_\eta}{\sqrt{s}} \int_0^{2\pi} d\phi_\eta \int_{-1}^{1} d\cos\theta_\eta \times \int_0^{2\pi} d\tilde{\phi} \int_{-1}^{1} d\cos\tilde{\theta} \overline{\sum} \sum |T_{\gamma p \to \eta \pi^0 p}|^2 \quad (5)$$

with $M_f = M_p$ and $\tilde{p}_\pi$ the modulus of the momentum $\tilde{\boldsymbol{p}}_\pi$ of the π^0 in the $\pi^0 p$ rest-frame,

$$\tilde{p}_\pi = \frac{1}{2M_I}\lambda^{1/2}(M_I^2, m_\pi^2, M_p^2) \tag{6}$$

where $\lambda^{1/2}(a^2, b^2, c^2) = \sqrt{[a^2-(b+c)^2][a^2-(b-c)^2]}$ is the Källén function and the direction of $\tilde{\boldsymbol{p}}_\pi$ is given by $\tilde{\phi}$ and $\tilde{\theta}$. This vector is connected to $\boldsymbol{p}_\pi$ in the γp rest-frame by the boost

$$\boldsymbol{p}_\pi = \left[\left(\frac{\sqrt{s}-\omega_\eta}{M_I} - 1\right)\left(-\frac{\tilde{\boldsymbol{p}}_\pi \boldsymbol{p}_\eta}{\boldsymbol{p}_\eta^2}\right) + \frac{\tilde{p}_\pi^0}{M_I}\right](-\boldsymbol{p}_\eta) + \tilde{\boldsymbol{p}}_\pi \tag{7}$$

where $\tilde{p}_\pi^0 = \sqrt{\tilde{\boldsymbol{p}}_\pi^{\,2} + m_\pi^2}$. The η three-momentum in Eq. (5) is in the overall c.m. frame of γp and is given by $p_\eta = \lambda^{1/2}(s, M_I^2, m_\eta^2)/(2\sqrt{s})$ and the two angles ϕ_η, θ_η. The $\overline{\sum}\sum$ denotes the usual average and sum over the initial and the final states, respectively.

The parameterization of the cross section in this way allows for the calculation of the $\pi^0 p$ invariant mass distribution, but not, e.g., for the other 2 cases of invariant masses, which would require a re-parameterization of the amplitude and phase space integrals.

However, the integral can be solved by Monte Carlo integration which allows for a relatively easy evaluation of other observables. For this, it is advantageous to rewrite the integration over dM_I in terms of dp_η by means of

$$M_I^2(\pi^0 p) = s + m_\eta^2 - 2\sqrt{s}\sqrt{m_\eta^2 + p_\eta^2}. \tag{8}$$

Then, evenly distributed random events are generated for all five integration variables p_η, ϕ_η, θ_η, $\tilde{\phi}$, and $\tilde{\theta}$ within their limits given in Eq. (5) (the limits of the p_η integration are $p_\eta \in [0,\, \lambda^{1/2}(s, (m_\pi + M_p)^2, m_\eta^2)/(2\sqrt{s})]$).

A random event (j) is given by a set of these five values $(p_\eta^{(j)},\, \phi_\eta^{(j)},\, \theta_\eta^{(j)},\, \tilde{\phi}^{(j)}, \tilde{\theta}^{(j)})$ and the corresponding contribution to the phase space integral,

$$R^{(j)} = \left(\frac{\sqrt{s}}{M_I(\pi^0 p)}\,\frac{p_\eta^{(j)}}{\omega_\eta}\right)\,\frac{1}{4(2\pi)^5}\frac{M_p M_f}{s-M_p^2}\,\frac{\tilde{p}_\pi p_\eta^{(j)}}{\sqrt{s}} \times \overline{\sum}\sum |T_{\gamma p\to\eta\pi^0 p}|^2(M_I(\pi^0 p), \theta_\eta^{(j)}, \phi_\eta^{(j)}, \tilde{\theta}^{(j)}, \tilde{\phi}^{(j)}) \tag{9}$$

where the first term in parenthesis comes from the change of integration from $M_I(\pi^0 p)$ to p_η. The quantities ω_η, $M_I(\pi^0 p)$, and $\tilde{p}_\pi$ can all be expressed in terms of the five integration variables, as previously given.

The total cross section is evaluated with a Monte Carlo integral that is given by the sum over events $R^{(j)}$, multiplied with the integration ranges for each variable, and divided by the number of events N,

$$\sigma = \frac{1}{N}\sum_{j=1}^{N} E^{(j)},$$
$$E^{(j)} = (2\pi)^2\, 2^2\, \frac{1}{2\sqrt{s}}\, \lambda^{1/2}(s, m_\pi + M_p, m_\eta)\, R^{(j)}. \tag{10}$$

Note that for the present study, we need an event set of polarized photons instead of unpolarized ones. The reaction amplitude can be written explicitly as $T_i = \hat{\boldsymbol{\epsilon}}_i \cdot \boldsymbol{T}$ where i stands for the polarization vectors in x and y direction. To get the total unpolarized cross section, one sums over i; thus, one obtains events polarized in the y direction by restricting the sum to the term $T_{i=y}$. Note that a factor of two has to be supplied to the cross section for polarized photons (compared to the unpolarized case) from the average over initial states $\overline{\sum}$ of Eq. (5).

With the method described above, it is now easy to evaluate many observables, because the only remaining task is to bin the random events $R^{(j)}$ to the bins of the desired observable, and those bins can be uniquely constructed from $(p_\eta^{(j)},\, \phi_\eta^{(j)},\, \theta_\eta^{(j)},\, \tilde{\phi}^{(j)}, \tilde{\theta}^{(j)})$ for each event.

For example, for the calculation of I^S and I^C, $N = 4.8 \cdot 10^5$ random events are binned in 16×16 bins for ϕ and ϕ^*. For this, the three-vectors of the p, π^0, and η in the overall c.m. system are reconstructed for each event from the five variables and using Eq. (7). Then, $\phi^{(j)}$ and $(\phi^*)^{(j)}$ are calculated from the equations given in Sec. 2.1 for each event.

Finally, the binned double differential cross section for the bins ϕ_i and ϕ_k^* is given by

$$\frac{d^2\sigma(\phi,\phi^*)}{d\phi\, d\phi^*} \simeq \frac{\Delta^2\sigma(\phi_i,\phi_k^*)}{\Delta\phi\,\Delta\phi^*} = \sum_{j=1}^{N}\frac{E^{(j)}\, f(i,j,k)}{\Delta\phi\,\Delta\phi^*\, N} \tag{11}$$

with the weight $E^{(j)}$ from Eq. (10), the bin widths $\Delta\phi$ and $\Delta\phi^*$, and $f(i,j,k)$ a function which is one if the event angles $\phi^{(j)}$ and $(\phi^*)^{(j)}$ are simultaneously in the bins ϕ_i and ϕ_k^*, and zero otherwise. In practice, for each event of the Monte Carlo run we determine the range (denoted the box) of ϕ_i and ϕ_k^* where the event is generated and accumulate the values $E^{(j)}$ in the respective boxes, such that in one run one obtains the double differential cross section.

For fixed ϕ^* and a fully linearly polarized beam, the ϕ differential cross section obeys the ϕ dependence [28,36]

$$\frac{d\sigma}{d\phi} = \sigma_0[1 + I^S \sin(2\phi) + I^C \cos(2\phi)]. \tag{12}$$

The last step to obtain I^S and I^C as a function of ϕ^* is to fit the differential cross section of Eq. (11) with the ϕ distribution given in Eq. (12), separately for every ϕ^* bin.

One has to choose the binning slightly differently to evaluate another observable, measured in Ref. [35] and given by

$$I^\theta = \frac{d\Sigma}{d\,\cos\theta} \tag{13}$$

with θ being the polar angle of the spectator particle (cf. Fig. 3). For this, we construct a double differential cross section in analogy to Eq. (11),

$$\frac{d^2\sigma(\phi,\cos\theta)}{d\phi\, d\cos\theta} \simeq \frac{\Delta^2\sigma(\phi_i,(\cos\theta)_k)}{\Delta\phi\,\Delta\cos\theta} \tag{14}$$

and fit it for fixed $\cos\theta$ with the ansatz

$$\frac{d\sigma}{d\phi} = \sigma_0[1 + I^{S,\theta}\sin(2\phi) + I^{\theta}\cos(2\phi)] \qquad (15)$$

and for the three cases of the p, π^0, and η being the spectator.

The method described in this section has been tested extensively: Generating events with unpolarized photons: I^S and I^C are zero for all ϕ^*, as must be. Also, we have checked the results of the Monte Carlo method with the ηp invariant mass distribution and the total cross section, that can be evaluated without the Monte Carlo method (cf. Eq. (45) of Ref. [39]). In fact, in the same binning algorithm used to obtain I^S and I^C, the previously evaluated results from Refs [39,31] have been reproduced.

3 Results

The measurements of I^S and I^C from Ref. [36] are shown in Figs. 4 and 5 (filled circles). These polarization observables obey the symmetries $I^S(\phi^*) = -I^S(2\pi - \phi^*)$ and $I^C(\phi^*) = I^C(2\pi - \phi^*)$ [36]. The experimental data according to these relations are shown with the open circles in Figs. 4 and 5; the discrepancy to the original data set (filled symbols) is within the statistical error estimated in Ref. [36].

The results of the present study for I^S and I^C are shown in Figs. 4 and 5 with the (red) solid lines [1], together with the data from Ref. [36]. At a given total energy $W \equiv \sqrt{s}$, $4.8{\cdot}10^5$ Monte Carlo events have been binned in $16{\times}16$ bins for ϕ and ϕ^*, and the quantities I^S and I^C have been obtained by fitting the ϕ distributions as described in the previous section. The binning is clearly visible in Figs. 4 and 5, for which the theoretical results for the 16 ϕ^* bins have been connected with piecewise straight lines.

The agreement with the data in Figs. 4 and 5 is good for the two lower energies $W = 1706$ MeV and $W = 1834$ MeV, given that the theoretical curves are predictions of the model from Refs. [39,48]. For the highest energy $W = 1946$ MeV, deviations of the prediction from the data start to become noticeable in $I^S_{\pi^0}$, I^S_η and I^C_η, while I^S_p and I^C_p are still well predicted. This is a sign that at higher energies new mechanisms start to become important which are not considered in Refs. [39,48]. This could, e.g., be a $\Delta(1940)\,D_{33}$ resonance which was needed in the Bonn-Gatchina partial wave analysis of the same reaction in Ref. [32]. Also, the $a_0(980)p$ final state, which is not included in the present model, can play a role at higher energies. It has been clearly seen at high energies in invariant mass distributions of the reaction [54].

[1] Note that for the lowest energy $W = 1706$ MeV, the theoretical total cross section is raising much faster than linear [31], and the model has not been evaluated at the center of the experimental bin at $W = 1706$ MeV, but at $W = 1740$ MeV which corrects for the finite experimental bin width. The value of $W = 1740$ MeV has been obtained by calculating the expectation value of k_γ, using the theoretical total cross section in the experimental bin over the energy range of 1706 ± 64 MeV.

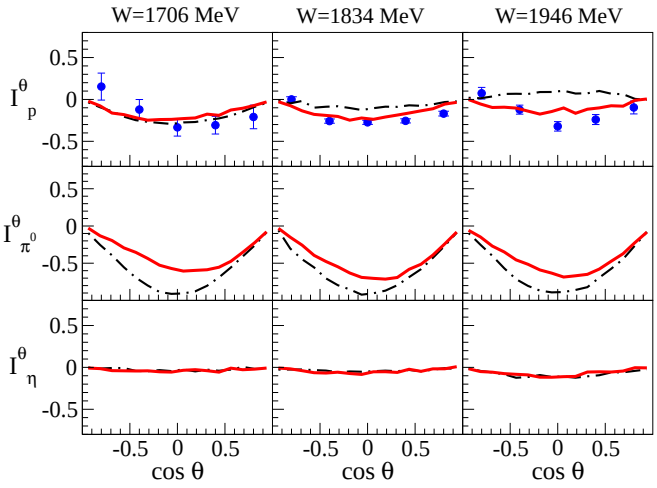

Fig. 6. (Color online) Polarization observable $I^\theta(\cos\theta) = \frac{d\Sigma}{d\cos\theta}$ for the three cases of p, π^0, and η spectators and for three different energies $W \equiv \sqrt{s}$. The data are from Ref. [35]. (Red) solid lines: Present results predicted from the model of Refs. [39,48]. (Black) dash-dotted lines: Only contribution from Fig. 1.

To test the sensitivity of different processes to I^S and I^C, we have removed parts of the theoretical model and re-evaluated I^S and I^C. From the list of processes discussed in Ref. [39], the ones shown in Figs. 1 and 2 are of special interest, because they contain the non-trivial predictions of the chiral unitary model of Ref. [45] for the large, complex coupling constants of the $\Delta(1700)$ to $\eta\Delta$ and $K\Sigma(1385)$. Omitting these processes, the (black) dotted lines in Figs. 4 and 5 are obtained, in gross disagreement with the data. This shows that these processes are indeed responsible for the ϕ^* dependence and the good agreement with the data. Note also that for the dotted curves, small effects of statistical noise become clearly visible, tied to the Monte Carlo based evaluation of the phase space integrals discussed in the previous section.

To test the sensitivity of the processes shown in Fig. 2, we have switched them off. The pertinent results are shown with the (green) dashed lines in Figs. 4 and 5 and turn out to be close to the full solution. This suggests that the process from Fig. 1 is dominant. The result from this process alone is shown with the (black) dash-dotted lines in Figs. 4 and 5. Indeed, the data are still qualitatively described, although the contribution from this process alone tends to overshoot the ϕ^* dependence of the result (cf., e.g., I^C_p at $W = 1834$ MeV and $W = 1946$ MeV). The latter finding implies that this process, although dominant, requires the presence of other processes with weaker ϕ^* dependence, such as given in Fig. 2 and also by the rest of the contributions discussed in Ref. [39] not displayed here but included. Then, the full solution, that contains all these processes and their interferences, leads to the good prediction of the data.

For completeness, also the observable $I^\theta = d\Sigma/d\cos\theta$, recently measured [35] by the CBELSA/TAPS collaboration, is evaluated in this study. In Ref. [35], also data

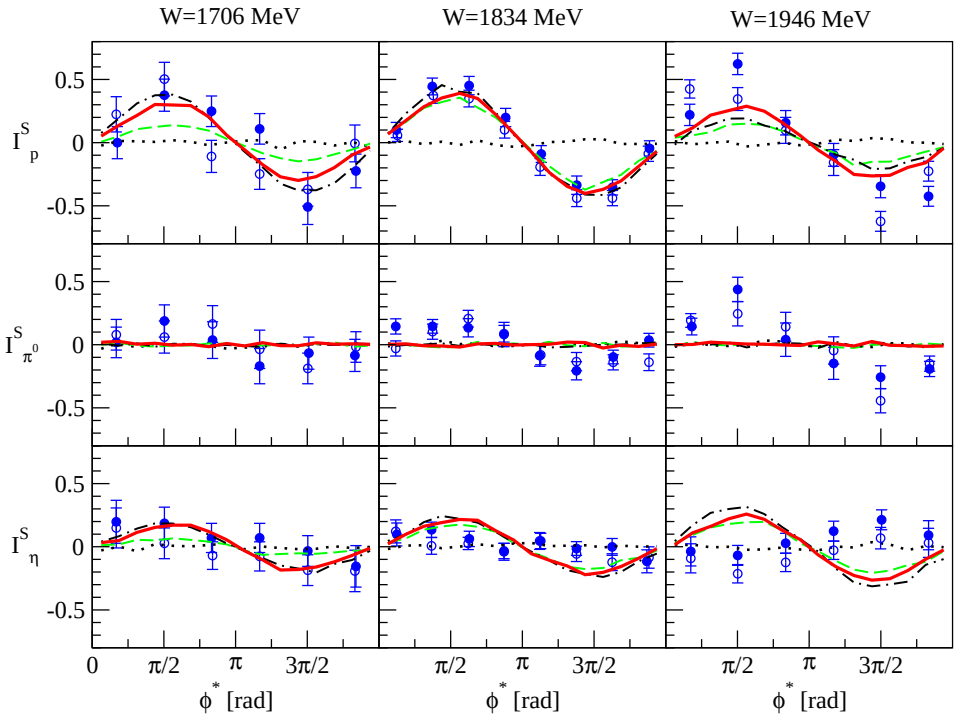

Fig. 4. (Color online) Polarization observable $I^S(\phi^*)$ for the three cases of p, π^0, and η spectators and for three different energies $W \equiv \sqrt{s}$. The data $I^S(\phi^*)$ are from Ref. [36] (full circles). The empty circles show $-I^S(2\pi - \phi^*)$. (Red) solid lines: Present results, predicted from the model of Refs. [39,48]. (Black) dotted lines: Without the $\Delta(1700)\eta\Delta$ and $\Delta(1700)K\Sigma(1385)$ couplings predicted from the chiral unitary model, i.e. without the processes from Figs. 1 and 2. (Green) dashed lines: Without the contributions from Fig. 2. (Black) dash-dotted lines: Only contribution from Fig. 1.

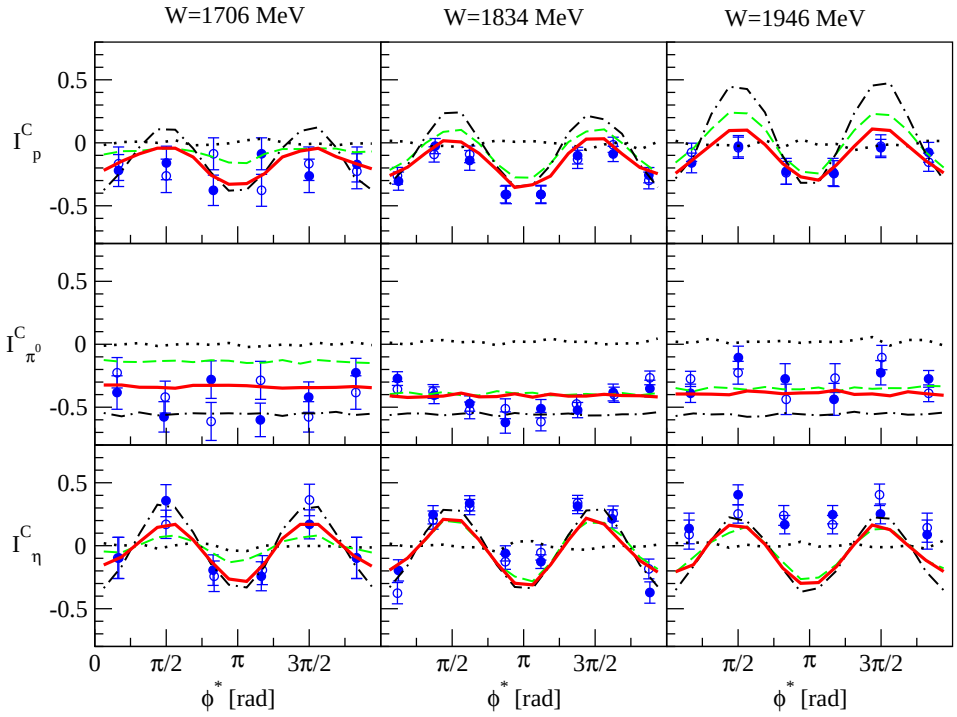

Fig. 5. (Color online) Polarization observable $I^C(\phi^*)$ for the three cases of p, π^0, and η spectators. The data $I^C(\phi^*)$ are from Ref. [36]. The empty circles show $I^C(2\pi - \phi^*)$. (Red) solid lines: Present results, predicted from the model of Refs. [39,48]. The other curves are labeled as in Fig. 4.

on the distributions $d\Sigma/d\,M_I$ were provided, in general agreement with the measurements by the GRAAL collaboration in Ref. [31] where one can also find the theoretical results of the present model for $d\Sigma/d\,M_I$.

The results of the present model for I^θ [cf. Eqs. (13, 15)] are shown in Fig. 6 (red solid lines). Also, the distributions for the π^0 and η spectator cases are shown, where no data are provided in Ref. [35]. The distributions for these two cases have already been analyzed and will be published in the near future [55].

The model describes the data quite well, although at the highest energy, clear deviations become noticeable, which was also the case for I^S and I^C shown before. The contribution from the diagram of Fig. 1 alone is shown by the (black) dash-dotted lines. The proton spectator case I^θ_p is of special interest, because unlike in the case of I^S and I^C, at the energy of $W = 1834$ MeV the contribution

from Fig. 1 is small and the result comes mainly from the other processes of the model of Ref. [39]. This clearly shows that there are processes beyond the one of Fig. 1, and the binning in $\cos\theta$ is sensitive to them.

The results for the polarization $I^{S,\theta}$, defined in Eq. (15), are zero within the statistics provided by the Monte Carlo evaluation. This has been also found in experiment [35].

3.1 Systematic uncertainties

It is of utmost importance to discuss the theoretical uncertainty of the results discussed so far, because only then one can truly speak of agreement (or disagreement) with the data. This is usually the hardest part of the theoretical calculation. For the case at hand, systematic theoretical errors can only be estimated, as we discuss in what follows. Most interesting is the dependence on the couplings of the $\Delta(1700)$ to the $\eta\Delta$ and $K\Sigma(1385)$ channels, $g_{\eta\Delta} = 1.7 - 1.4\,i$, $g_{K\Sigma(1385)} = 3.3 + 0.7\,i$, which are predictions of the chiral unitary model of Ref. [45].

In Ref. [46], this model has been improved by the inclusion of the πN channel in D-wave and a fit of the subtraction constants to the πN D_{33} phase shift of Ref. [56]. The updated values of the coupling constants from Ref. [46] are $g_{\eta\Delta} = -2.27 - 1.89\,i$, $g_{K\Sigma(1385)} = 3.01 + 1.95\,i$. We have evaluated the asymmetries I^S, I^C, and I^θ at the energy $W = 1834$ MeV with these updated values. The result is shown in Fig. 7 with the (indigo) dash-double dotted lines. Although the updated couplings g are quite different from the original values, the asymmetries I are almost unchanged: For I^S and I^C, the process of Fig. 1 is dominant, and the contributions to I^S and I^C from this diagram alone are independent of the value of the coupling $g_{\eta\Delta}$ as the definition of Eq. (12) shows and taking into account that $g_{\eta\Delta}$ factorizes in the amplitude of Fig. 1. Note, however, that $g_{\eta\Delta}$ and $g_{K\Sigma(1385)}$ also appear in the rescattering diagrams shown in Fig. 2, but their influence on I^S and I^C is small.

Another source of uncertainty is the coupling of the photon to the $\Delta(1700)$, as shown in Fig. 1. The $\gamma N\Delta(1700)$ phototransition is given by the helicity amplitudes $A_{1/2} = 0.104 \pm 0.015$ GeV$^{-1/2}$ and $A_{3/2} = 0.085 \pm 0.022$ GeV$^{-1/2}$ at the photon point $Q^2 = 0$ [47]. These values translate into the couplings g_1' and g_2' in the amplitude [cf. Eqs. (39,43) of Ref. [39]]. As in case of the strong couplings g discussed above, for the process from Fig. 1 the asymmetries I do not depend on the overall magnitude of the $\gamma N\Delta(1700)$ coupling, but only on the ratio $g_1'/g_2' = -0.26 M_N^{-1}/(+0.27 M_N^{-2})$ [23,39]. The mentioned uncertainties in $A_{1/2}$ and $A_{3/2}$ translate into an estimated uncertainty of about 22% for the ratio g_1'/g_2'. Evaluating the process of Fig. 1 with the ratios $g_1'/g_2'(1 \pm 0.22)$, we obtain the (yellow) bands shown in Fig. 7. The result with the unchanged ratio g_1'/g_2' is shown with the (black) dash-dotted lines. As the figures shows, the uncertainty from this source is well controlled.

Summarizing, we have shown that the $\Delta(1700)$ photoexcitation with subsequent decay into $\eta\Delta$ as shown in Fig. 1 is the most important contribution to I^S and I^C; however, we have also seen that the asymmetries I^S and I^C from this process are insensitive to the size of the $\gamma N\Delta(1700)$ and $\Delta(1700)\eta\Delta$ couplings, and that systematic uncertainties in these couplings are well controlled.

3.2 Interconnections with other experiments

One should see the present results also in perspective to the previously evaluated observables from Refs. [39,48,31]. In the first work of Ref. [39], where the theoretical framework was developed, the total cross section and invariant masses were predicted. While at the lowest energies the theoretical cross section is slightly below the data [31], the overall agreement is good, in particular also for the case of the related reaction $\gamma p \to \pi^0 K^0 \Sigma^+$: the predictions for the differential and total cross sections have been experimentally confirmed recently in Ref. [49].

However, for some of the ηp invariant masses in $\gamma p \to \pi^0 \eta p$, deviations from the data have been observed in Ref. [31], which are most probably tied to a too narrow $N(1535)$ which also appears dynamically generated in the present model, based on the study of Ref. [57]. This problem appears also in the different context of single pion photoproduction and has been recently addressed in Refs. [58, 59]. It was traced back to the absence of the $N(1650)\,S_{11}$ resonance in the original model [57] which was then included in Ref. [58] and led to a consistent description of pion- and photon-induced single pion production. An upgrade of the present model for $\gamma p \to \pi^0 \eta p$ with these new results would be desirable.

For the other invariant masses in $\gamma p \to \pi^0 \eta p$, in particular $M_I(\pi^0\eta)$, better agreement with the GRAAL experiment has been observed in Ref. [31]. There, also the predictions for the beam asymmetries $d\Sigma/dM_I$ have been compared to experiment and an overall agreement could be found. Note that the beam asymmetries Σ, which have also been measured in the CBELSA/TAPS experiment [35], correspond to I^C if the dependence on ϕ^* is integrated out, as has been pointed out in Refs. [36,54].

The formalism developed in Ref. [39] has also been applied to other reactions in Ref. [48]. In particular, the predicted [45] $\Delta(1700)$ couplings to $\eta\Delta$, $K\Sigma(1385)$, and $\pi\Delta$ could be used to evaluate eleven different pion- and photon-induced reactions resulting in an overall agreement, although for some of the reactions studied, some extra ingredients would be needed at higher energies, where a strong forward peaking of some differential cross sections becomes noticeable.

4 Conclusions

The theoretical predictions of I^S, I^C, and I^θ in the $\gamma p \to \pi^0 \eta p$ reaction, evaluated from a chiral unitary model, agree well with the data recently measured at CBELSA/TAPS. We have shown that from the list of processes discussed in Ref. [39], the photon excitation of the $\Delta(1700)$ with subsequent S-wave decay into $\eta\Delta$ is mainly responsible

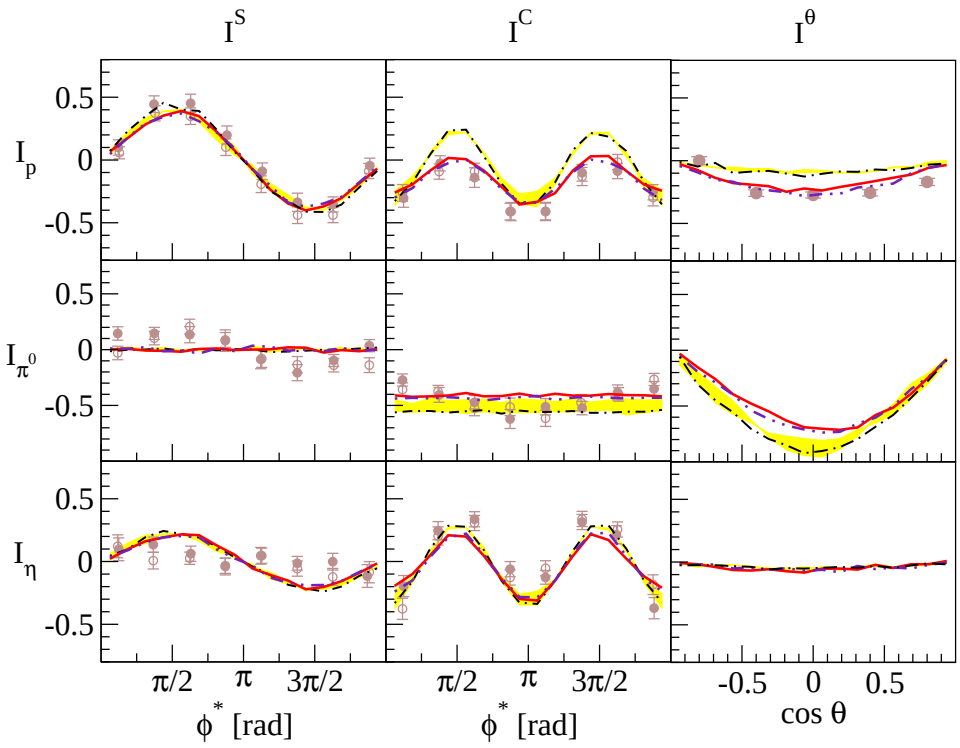

Fig. 7. (Color online) Estimate of the systematic error of the present model at $W = 1834$ MeV. The (red) solid lines show the result of the full model of Ref. [39], the (indigo) dash-double dotted lines the full model, but with the updated $\Delta(1700)\eta\Delta$ and $\Delta(1700)K\Sigma(1385)$ coupling constants from Ref. [46]. The (black) dash-dotted lines show the contribution from Fig. 1. The (yellow) bands show the uncertainties of this contributions induced from the experimental uncertainties of the photon coupling of the $\Delta(1700)$.

for the ϕ^* dependence. The $\Delta(1700)$ couplings to $\eta\Delta$, $K\Sigma(1385)$, and $\pi\Delta$ are predictions from a chiral unitary model in which the $\Delta(1700)$ appears dynamically generated from the unitarized interaction of the octet of $J^P = 1/2^-$ mesons with the decuplet of $J^P = 3/2^+$ baryons. The present results provide further evidence for this concept, which had been previously tested and verified for other observables in $\gamma p \to \pi^0 \eta p$ and also in ten other pion- and photon-induced reactions.

This work is partly supported by DGICYT and FEDER funds Contract No. FIS 2006-03438, the Generalitat Valenciana in the program Prometeo and the EU Integrated Infrastructure Initiative Hadron Physics Project under contract RII3-CT-2004-506078. This work is also supported by the DFG (Deutsche Forschungsgemeinschaft, Gz: DO 1302/1-2 and SFB/TR-16). We would like to thank E. Gutz for providing the information on the definitions of the reaction geometry, useful discussions, and a careful reading of the manuscript.

References

1. A. Braghieri *et al.*, Phys. Lett. B **363**, 46 (1995).
2. A. Zabrodin *et al.*, Phys. Rev. C **55**, 1617 (1997).
3. F. Härter *et al.*, Phys. Lett. B **401**, 229 (1997).
4. A. Zabrodin *et al.*, Phys. Rev. C **60**, 055201 (1999).
5. M. Wolf *et al.*, Eur. Phys. J. A **9**, 5 (2000).
6. W. Langgartner *et al.*, Phys. Rev. Lett. **87**, 052001 (2001).
7. Y. Assafiri *et al.*, Phys. Rev. Lett. **90**, 222001 (2003).
8. M. Ripani *et al.* [CLAS Collaboration], Phys. Rev. Lett. **91**, 022002 (2003).
9. J. Ahrens *et al.* [GDH and A2 Collaborations], Phys. Lett. B **551**, 49 (2003).
10. M. Kotulla *et al.*, Phys. Lett. B **578**, 63 (2004).
11. J. Ahrens *et al.* [GDH and A2 Collaborations], Phys. Lett. B **624**, 173 (2005).
12. S. Strauch *et al.* [CLAS Collaboration], Phys. Rev. Lett. **95**, 162003 (2005).
13. J. Ahrens *et al.* [GDH and A2 Collaborations], Eur. Phys. J. A **34**, 11 (2007).
14. U. Thoma *et al.*, Phys. Lett. B **659**, 87 (2008).
15. A. V. Sarantsev *et al.*, Phys. Lett. B **659**, 94 (2008).
16. M. Battaglieri *et al.* [CLAS Collaboration], Phys. Rev. D **80**, 072005 (2009).
17. D. Krambrich *et al.* [Crystal Ball at MAMI Collaboration, TAPS Collaboration and A2 Collaboration], Phys. Rev. Lett. **103**, 052002 (2009).
18. J. A. Gómez Tejedor and E. Oset, Nucl. Phys. A **571**, 667 (1994).
19. J. A. Gómez Tejedor and E. Oset, Nucl. Phys. A **600**, 413 (1996).
20. V. Bernard, N. Kaiser, U.-G. Meißner and A. Schmidt, Nucl. Phys. A **580**, 475 (1994).
21. V. Bernard, N. Kaiser and U.-G. Meißner, Phys. Lett. B **382**, 19 (1996).
22. V. Bernard, U.-G. Meißner and N. Kaiser, Phys. Rev. Lett. **74**, 1036 (1995).
23. J. C. Nacher, E. Oset, M. J. Vicente and L. Roca, Nucl. Phys. A **695**, 295 (2001).
24. J. C. Nacher and E. Oset, Nucl. Phys. A **697**, 372 (2002).
25. V. I. Mokeev *et al.*, Phys. Atom. Nucl. **64**, 1292 (2001) [Yad. Fiz. **64**, 1368 (2001)].
26. L. Roca, Nucl. Phys. A **748**, 192 (2005).
27. A. Fix and H. Arenhövel, Eur. Phys. J. A **25**, 115 (2005).
28. W. Roberts and T. Oed, Phys. Rev. C **71**, 055201 (2005).
29. H. Kamano, B. Juliá Díaz, T. S. Lee, A. Matsuyama and T. Sato, Phys. Rev. C **80**, 065203 (2009).
30. T. Nakabayashi *et al.*, Phys. Rev. C **74**, 035202 (2006).

31. J. Ajaka *et al.*, Phys. Rev. Lett. **100**, 052003 (2008).
32. I. Horn *et al.* [CB-ELSA Collaboration], Phys. Rev. Lett. **101**, 202002 (2008).
33. I. Horn *et al.* [CB-ELSA Collaboration], Eur. Phys. J. A **38**, 173 (2008).
34. V. L. Kashevarov, Eur. Phys. J. A **42**, 141 (2009).
35. E. Gutz *et al.* [CBELSA/TAPS Collaboration], Eur. Phys. J. A **35**, 291 (2008).
36. E. Gutz *et al.* [CBELSA/TAPS Collaboration], Phys. Lett. B **687**, 11 (2010).
37. V. L. Kashevarov *et al.* [A2 Collaboration], arXiv: 1009.4093 [nucl-ex].
38. D. Jido, M. Oka and A. Hosaka, Prog. Theor. Phys. **106**, 873 (2001).
39. M. Döring, E. Oset and D. Strottman, Phys. Rev. C **73**, 045209 (2006).
40. M. Nanova and V. Metag, private communication.
41. A. Fix, M. Ostrick and L. Tiator, Eur. Phys. J. A **36**, 61 (2008).
42. A. Anisovich, E. Klempt, A. Sarantsev and U. Thoma, Eur. Phys. J. A **24**, 111 (2005).
43. A. V. Anisovich, V. Kleber, E. Klempt, V. A. Nikonov, A. V. Sarantsev and U. Thoma, Eur. Phys. J. A **34**, 243 (2007).
44. E. E. Kolomeitsev and M. F. M. Lutz, Phys. Lett. B **585**, 243 (2004).
45. S. Sarkar, E. Oset and M. J. Vicente Vacas, Nucl. Phys. A **750**, 294 (2005) [Erratum-ibid. A **780**, 78 (2006)].
46. M. Döring, Nucl. Phys. A **786**, 164 (2007).
47. C. Amsler *et al.* [Particle Data Group], Phys. Lett. B **667**, 1 (2008).
48. M. Döring, E. Oset and D. Strottman, Phys. Lett. B **639**, 59 (2006).
49. M. Nanova *et al.* [CBELSA/TAPS Collaboration], Eur. Phys. J. A **35**, 333 (2008).
50. A. Fix, V. L. Kashevarov, A. Lee and M. Ostrick, Phys. Rev. C **82**, 035207 (2010).
51. B. Borasoy, P. C. Bruns, U.-G. Meißner and R. Nißler, Phys. Rev. C **72**, 065201 (2005).
52. B. Borasoy, P. C. Bruns, U.-G. Meißner and R. Nißler, Eur. Phys. J. A **34**, 161 (2007).
53. J. C. Nacher, E. Oset, H. Toki and A. Ramos, Phys. Lett. B **461**, 299 (1999).
54. E. Gutz, private communication.
55. CBELSA/TAPS, publication in preparation.
56. R. A. Arndt, W. J. Briscoe, I. I. Strakovsky and R. L. Workman, Phys. Rev. C **74**, 045205 (2006).
57. T. Inoue, E. Oset and M. J. Vicente Vacas, Phys. Rev. C **65**, 035204 (2002).
58. M. Döring and K. Nakayama, Eur. Phys. J. A **43**, 83 (2010).
59. M. Döring and K. Nakayama, Phys. Lett. B **683**, 145 (2010).